Pointwise a posteriori error bounds for blow-up in the semilinear heat equation

Kyza, Irene; Metcalfe, Stephen

Published in:
SIAM Journal on Numerical Analysis

DOI:
10.1137/19M1264758

Publication date:
2020

Document Version
Peer reviewed version

POINTWISE A POSTERIORI ERROR BOUNDS FOR BLOW-UP IN THE SEMILINEAR HEAT EQUATION

IRENE KYZA AND STEPHEN METCALFE

Abstract. This work is concerned with the development of an adaptive space-time numerical method, based on a rigorous *a posteriori* error bound, for the semilinear heat equation with a general local Lipschitz reaction term whose solution may blow-up in finite time. More specifically, conditional *a posteriori* error bounds are derived in the $L^\infty L^\infty$ norm for the first order (Euler) in time, implicit-explicit (IMEX), conforming finite element method in space discretization of the problem. Numerical experiments applied to both blow-up and non blow-up cases highlight the generality of our approach and complement the theoretical results.

1. Introduction

Let $\Omega \subset \mathbb{R}^d$ with $d = 2$ or $d = 3$ be a bounded polyhedral domain and consider the problem

$$\begin{aligned} u_t - a\Delta u - f(u) &= 0 \qquad \text{in } \Omega,\ t > 0, \\ u &= 0 \qquad \text{on } \partial\Omega,\ t > 0, \\ u(\cdot, 0) &= u_0 \qquad \text{in } \Omega, \end{aligned} \tag{1.1}$$

where a is a positive constant and the initial condition $u_0 \in W^{2,\infty}(\Omega)$. Note that here the reaction term f can be both space and time dependent but as the nature of the dependence is usually clear, we omit writing it explicitly for brevity. It is well known that for certain data the solution to (1.1) exhibits *finite time blow-up* [19], that is, there exists a maximal time of existence $T_\infty < \infty$ referred to as the *blow-up time* such that (1.1) holds and

$$\|u(t)\|_{L^\infty(\Omega)} < \infty \text{ for } 0 < t < T_\infty, \qquad \lim_{t \nearrow T_\infty} \|u(t)\|_{L^\infty(\Omega)} = \infty.$$

If the solution to (1.1) does not exhibit finite-time blow-up then the solution is global and so $T_\infty = \infty$. Either way, we assume that (1.1) holds on some closed interval $[0, T]$ and that $T < T_\infty$. We will see in the sequel that we can show that (1.1) has a unique local solution $u \in C(0, T; L^\infty(\Omega))$ provided that an implicit *local a posteriori criteron* is satisfied and that this local critereon is robust with respect to the distance from the blow-up time.

The numerical approximation of blow-up phenomena in partial differential equations (PDEs) is a challenging problem due to the high spatial and temporal resolution needed close to the blow-up time. In the literature, there exist several *ad-hoc* numerical algorithms that produce good approximations to solutions of problems of the form (1.1) close to the blow-up time; see, for example, Acosta *et al.* [1], Berger/Kohn [7] and Nguyen/Zaag [35]. Based on the moving mesh PDE method (MMPDE), Budd *et al.* also propose such algorithms, cf. [8, 20] and the references therein while Groisman proposes an adaptive algorithm in [17] that is based on the asymptotic behavior of the exact solution. In all these works, information on the qualitative behavior of the exact solution close to the blow-up time is necessary; in fact, the aforementioned algorithms are driven by such behavior.

Recently, there has been a lot of interest [9, 25] in deriving rigorous a *posteriori* error bounds for problems of the form (1.1). Instead of relying on the qualitative behavior of the exact solution, the resulting estimators are used in oder to design an efficient adaptive procedure that will allow

2010 *Mathematics Subject Classification.* 65J08, 65L05, 65L60.

Key words and phrases. Semilinear heat equation, IMEX method, conditional *a posteriori* error estimates, blow-up singularities.

The authors acknowledge the support from the Carnegie Trust Research Incentive Grant RIG008215. S. Metcalfe acknowledges the support of the Swiss National Science Foundation (SNF) grant no. 200021-162990.

to get close to the blow-up time [9]. Indeed, it is easy to see why such an approach can confer significant advantages; for example, if it is known that the $L^\infty L^\infty$ norm of the error is always bounded from above by a finite quantity then it is impossible to surpass the blow-up time!

A posteriori error estimators for linear problems tend to be *unconditional*, that is, they always hold independent of the problem data and the size of the discretization parameters. For nonlinear problems, the situation is more complicated since the existence of a solution to an appropriate error equation (and, thus, of an error bound) usually requires that either the data or the discretization parameters are sufficiently small. As a result, *a posteriori* error estimators for nonlinear problems tend to be *conditional*, that is, they only hold provided that an *a posteriori* verifiable condition (which can be either explicit or implicit) is satisfied. For nonlinear time-dependent problems, there are two commonly used approaches for deriving conditional *a posteriori* error bounds: continuation arguments, cf. [6, 9, 11, 16, 21, 26, 31], and fixed point arguments, cf. [12, 24, 25, 32–34].

The derivation of such estimates for (1.1) and related problems in the context of blow-up was first explored in [24,25] for polynomial nonlinearities but these early pointwise bounds are not well suited for the practical computation of blow-up problems by virtue of being *global* rather than *local* in nature. The situation was improved in [9, 31] by the derivation of error bounds using energy techniques combined with the Gagliardo-Nirenberg inequality that are valid under local rather than global conditions. While the bounds of [9, 31] represent a significant improvement from a practical perspective, the derived error bounds still have significant drawbacks; for example, the range of nonlinearities that can be considered is smaller than in [24,25] due to Sobolev embedding restrictions and convergence towards the blow-up time is still *slow* when compared with results on the numerical approximation of blow-up in corresponding ODE cases [9, 26, 31]. It should be remarked, though, that the use of energy techniques in [9, 31] does confer advantages in other areas; specifically, it allows for the derivation of error bounds for problems with non-symmetric spatial operators, e.g., for problems which include advective terms.

In this paper, we seek to derive conditional *a posteriori* error bounds in the $L^\infty L^\infty$ norm for a fully discrete approximation of (1.1) where for the time discretization we use a first order (Euler) implicit-explicit (IMEX) method while for the spatial discretization we use the conforming finite element method. It is worth noting that the choice of an IMEX method not only confers advantages in terms of ease of solubility but has also been shown to have advantages in the context of estimation of the blow-up time, cf. [9, 31]. The results that we will present here are an improvement over existing results in the literature in two major ways. Firstly, we significantly broaden the range of nonlinearities under consideration; specifically, the (possibly) nonlinear reaction term $f : \bar{\Omega} \times [0, T_\infty) \times \mathbb{R} \to \mathbb{R}$ is assumed to be continuous and to satisfy the *local* Lipschitz estimate

$$|f(x,t,v) - f(x,t,w)| \leq \mathcal{L}(t, |v|, |w|)|v - w| \qquad \forall x \in \bar{\Omega} \quad \forall t \in [0, T_\infty) \quad \forall v, w \in \mathbb{R}. \tag{1.2}$$

Here, $\mathcal{L} : [0, T_\infty) \times \mathbb{R}_0^+ \times \mathbb{R}_0^+ \to \mathbb{R}_0^+$ is a *known* function that satisfies $\mathcal{L}(\cdot, a, b) \in L^1(0, T_\infty)$ for any $a, b \in \mathbb{R}_0^+$ and that is continuous and monotone increasing in the second and third arguments. This condition on f is quite general and includes many nonlinearities of interest, for example, it covers any polynomial nonlinearity with suitably regular coefficients as well as nonlinearities of exponential type [26]. We stress that this local Lipschitz assumption is in contrast to assumptions made for currently existing pointwise *a posteriori* bounds of (1.1), cf. [22, 23], wherein the focus is on the singularly preturbed case and, thus, f is assumed to be globally Lipschitz. Secondly, we follow the approach taken in [22–25] of conducting the error analysis via semigroup techniques – this allows us to consider the error in an ODE setting. In combination with a *local-in-time* fixed point argument along the lines of [26], this restores the optimality that is otherwise lost in an energy setting [9, 31]. Additionally, we show numerically that our conditional *a posteriori* error bound is well-behaved with respect to the distance from the blow-up time; specifically, we show that the rate of convergence to the blow-up time is comparable to the rate observed in [9, 26, 31]. Finally, we stress out that our error estimator is valid not only for problems with finite time blow-up but for any problem of the form (1.1) satisfying (1.2) – we illustrate this in the last numerical experiment where we consider a problem without blowup but with boundary layers instead.

Outline. We begin in Section 2 by outlining the fully discrete IMEX finite element discretization of (1.1) then in Section 3 we introduce several auxiliary results which will be used in the error analysis. In Section 4, we derive the conditional *a posteriori* error bound and in Section 5 we propose a general adaptive algorithm, applicable to both blow-up and fixed-time problems (i.e., for problems without finite time blow-up), that is based upon the derived *a posteriori* error bound. We apply this adaptive algorithm to several numerical examples in Section 6 in order to illustrate that the proposed *a posteriori* bound is well-behaved close to the blow-up time. Finally, we draw conclusions and outline our plans for future research in Section 7.

Notation. As they will be used frequently in this work, we denote the L^2 inner product on Ω by $(\cdot,\cdot)$ and the L^∞ norm on Ω by $||\cdot||$.

2. Discretization

Consider a shape-regular mesh $\mathcal{T}=\{K\}$ of Ω with K denoting a generic element of diameter h_K that is constructed via affine mappings $F_K:\widehat{K}\to K$ with non-singular Jacobian where $\widehat{K}$ is the d-dimensional reference simplex or the d-dimensional reference cube. The mesh is allowed to contain a uniformly fixed number of regular hanging nodes per face. With these definitions, the finite element space $\mathcal{V}_h(\mathcal{T})$ over the mesh $\mathcal{T}$ is given by

$$\mathcal{V}_h(\mathcal{T}):=\{v\in H_0^1(\Omega)\cap C(\Omega):v|_K\circ F_K\in\mathcal{P}^p(\widehat{K}),\,K\in\mathcal{T}\},\tag{2.1}$$

where $\mathcal{P}^p(\widehat{K})$ denotes the space of polynomials of total degree p if $\widehat{K}$ is the d-dimensional reference simplex or of degree p in each variable if $\widehat{K}$ is the d-dimensional reference cube. Given two meshes $\mathcal{T}_1$ and $\mathcal{T}_2$, we denote their *coarsest common refinement* by $\mathcal{T}_1\vee\mathcal{T}_2$ and their *finest common coarsening* by $\mathcal{T}_1\wedge\mathcal{T}_2$. We also define the jump residual $[\![\nabla v_h]\!]$ of a function $v_h\in\mathcal{V}_h(\mathcal{T})$ at a point x on the $(d-1)$-dimensional inter-element face $E=\bar{K}\cap\bar{K}'$, $K,K'\in\mathcal{T}$ by

$$[\![\nabla v_h]\!](x):=\lim_{\delta\to 0}[\nabla v_h(x+\delta n)-\nabla v_h(x-\delta n)]\cdot n,$$

where n is an arbitrary unit normal vector on E.

We consider the first order in time, IMEX, space-time discretization of (1.1) consisting of implicit treatment for the diffusion term and explicit treatment for the nonlinear reaction term. For the spatial discretization, we use the standard conforming finite element method. To this end, we introduce a sequence of time nodes $0:=t_0<t_1<\cdots<t_{M-1}<t_M:=T$ which induces a partition of $[0,T]$ and let $I_m:=(t_{m-1},t_m)$, $m=1,\ldots,M$. The length $k_m:=t_m-t_{m-1}$ (which may be variable) of the time interval I_m is called the time step length. If we let $\mathcal{T}_1$ denote an initial spatial mesh of Ω associated with the first time interval I_1 then to each successive time interval I_m, $m=2,\ldots,M$, we associate a spatial mesh $\mathcal{T}_m$ which is assumed to have been obtained from $\mathcal{T}_{m-1}$ by local refinement and/or coarsening. We remark that this restriction upon mesh change is made in order to avoid degradation of the finite element solution, cf. [5, 15]. To each mesh $\mathcal{T}_m$ we then assign the finite element space $\mathcal{V}_h^m:=\mathcal{V}_h(\mathcal{T}_m)$, $m=1,\ldots,M$, given by (2.1).

With this notation at hand, the IMEX fully discrete finite element method reads as follows: we seek $U^m\in\mathcal{V}_h^m$, $m=1,\ldots,M$, such that

$$\left(\frac{U^m-U^{m-1}}{k_m},V^m\right)+a(\nabla U^m,\nabla V^m)-(f^{m-1},V^m)=0\qquad\forall V^m\in\mathcal{V}_h^m,\tag{2.2}$$

holds where we set $f^{m-1}:=f(\,\cdot\,,t_{m-1},U^{m-1})$ for brevity and the initial value is given by $U^0:=\mathcal{P}^1u_0$ with $\mathcal{P}^1$ denoting the L^2-projection operator onto $\mathcal{V}_h^1$. For $t\in\bar{I}_m$, $m=1,\ldots,M$, $U(t)$ is then defined to be the linear interpolant with respect to t of the values U^{m-1} and U^m, viz.,

$$U(t):=\ell_{m-1}(t)U^{m-1}+\ell_m(t)U^m,$$

where $\{\ell_{m-1},\ell_m\}$ denotes the standard linear Lagrange interpolation basis on the interval $\bar{I}_m$, i.e., $\ell_{m-1}(t):=\frac{t_m-t}{k_m}$ and $\ell_m(t):=\frac{t-t_{m-1}}{k_m}$, $t\in\bar{I}_m$.

3. Error Analysis

Before we proceed with the error analysis, we require some auxiliary results and some additional notation. Our first result is a maximum principle for a related parabolic equation.

Theorem 3.1. *Let $\mathrm{e}^{t\Delta}$ be the solution operator for the problem*

$$\begin{aligned} w_t - a\Delta w &= 0 && \text{in } \Omega,\ t>0,\\ w &= 0 && \text{on } \partial\Omega,\ t>0,\\ w(\cdot,0) &= w_0 && \text{in } \Omega, \end{aligned}$$

with $w_0 \in L^\infty(\Omega)$. In other words, $w(t) = \mathrm{e}^{t\Delta}w_0$. Then for any $t>0$, the following bound holds

$$||\mathrm{e}^{t\Delta}w_0|| \leq ||w_0||.$$

Proof. See page 93 in [37]. □

We next introduce an error bound for a related elliptic problem which will be crucial in the error analysis of the parabolic problem.

Theorem 3.2. *Let $w \in H_0^1(\Omega)\cap C(\bar{\Omega})$ be the unique solution to the elliptic problem*

$$\begin{aligned} -a\Delta w &= g && \text{in } \Omega,\\ w &= 0 && \text{on } \partial\Omega, \end{aligned}$$

where $g \in C(\Omega)$ and let $w_h \in \mathcal{V}_h$ be its conforming finite element approximation. Then the following pointwise a posteriori bound holds

$$||w-w_h|| \leq C_\infty \log(1/\underline{h}) \max_{K\in\mathcal{T}} \left[h_K^2 a^{-1}||g+a\Delta w_h||_{L^\infty(K)} + h_K||[\![\nabla w_h]\!]||_{L^\infty(\partial K\setminus\partial\Omega)}\right],$$

where $\underline{h} := \min_{K\in\mathcal{T}} h_K$ is the minimum mesh-size and C_∞ is a positive constant that is independent of the maximum mesh-size, a, w and w_h but may be dependent upon the size of the domain Ω.

Proof. See [13]. □

Remark 3.3. The error bound of Theorem 3.2 and, thus, the spatial error estimators in the forthcoming parabolic error analysis are well-behaved in the elliptic regime but badly-behaved in the singularly preturbed regime ($a \approx 0$), cf. [13]. As we are primarily interested in blow-up in the elliptic regime, we elect to use the simpler error bound of Theorem 3.2 but if one is interested in the singularly preturbed regime, the spatial estimators should be replaced with the *full* estimator from [13].

In the forthcoming error analysis, on each time step m, we will work with the Banach space $C(\bar{I}_m; L^\infty(\Omega))$ – the space of all continuous functions $v : \bar{I}_m \to L^\infty(\Omega)$ equipped with the norm

$$||v||_m := \sup_{t\in\bar{I}_m} ||v(t)||.$$

In what follows, we will need to make use of the elliptic reconstruction technique originally introduced in [27, 28]. To that end, we define the *elliptic reconstruction* $\omega^m \in H_0^1(\Omega)$, $m = 1,\ldots,M$, to be the solution of

$$a(\nabla\omega^m, \nabla v) = (A^m, v) \qquad \forall v \in H_0^1(\Omega), \tag{3.4}$$

where $A^m := f^{m-1} - U_t\big|_{I_m}$. Note that the L^2-projection of A^m onto $\mathcal{V}_h^m$ is the discrete laplacian of aU^m hence our definition of the elliptic reconstruction is not exactly the same as in [27, 28] but is instead in the spirit of [14]. Note that with this definition, A^m has nonzero boundary values. This modification is used to maintain consistency in the pointwise analysis [14] and leads to better numerical results in the implementation of the spatial a posteriori error estimator. For $m = 0$, we set $\omega^0 := u_0$ and further define $A^0 := -a\Delta u_0$.

As with the numerical solution $U(t)$, $\omega(t)$ is defined to be the linear interpolant with respect to t of the values ω^{m-1} and ω^m, viz.,

$$\omega(t) := \ell_{m-1}(t)\omega^{m-1} + \ell_m(t)\omega^m, \tag{3.5}$$

for $t \in \bar{I}_m$, $m = 1, \ldots, M$. For the error analysis, the error $e := u - U$ will be decomposed $e = \rho + \epsilon$ where $\rho := u - \omega$ is the *parabolic error* and $\epsilon := \omega - U$ is the *elliptic error*. Note that for $m = 0$ we have $\rho(0) = 0$ and $\epsilon(0) = e(0) = u_0 - \mathcal{P}^1 u_0$ (which is a computable quantity) whereas for $m \geq 1$ we can estimate $||\epsilon(t_m)||$ via elliptic error estimators currently available in the literature (based on the observation that (2.2) is the conforming finite element discretization of the elliptic problem (3.4)). To that end, we have the following lemma.

Lemma 3.6. *For $m \geq 1$, the estimate*

$$||\epsilon(t_m)|| \leq \mathcal{E}_m := C_\infty \log(1/\underline{h}_m) \max_{K \in \mathcal{T}_m} \eta_S^m\big|_K,$$

holds with $\underline{h}_m := \min_{K \in \mathcal{T}_m} h_K$ denoting the minimum mesh-size, C_∞ the constant of Theorem 3.2 and where η_S^m is the primary space estimator given by

$$\eta_S^m\big|_K := h_K^2 a^{-1} ||A^m + a\Delta U^m||_{L^\infty(K)} + h_K ||[\![\nabla U^m]\!]||_{L^\infty(\partial K \setminus \partial\Omega)}, \qquad K \in \mathcal{T}_m.$$

Proof. Since $A^m \in C(\Omega)$, this follows directly from Theorem 3.2. □

To begin construction of the error equation, we first deduce from (3.4) and (3.5) that

$$-a\Delta\omega = \ell_{m-1} A^{m-1} + \ell_m A^m, \tag{3.7}$$

for any $t \in \bar{I}_m$. We then subtract (3.7) from (1.1) to obtain

$$u_t - a\Delta\rho = f(u) - \ell_{m-1} A^{m-1} - \ell_m A^m. \tag{3.8}$$

Adding and subtracting $f(\omega)$ and $f(U)$ then yields

$$u_t - a\Delta\rho = f(\rho + \omega) - f(\omega) + f(\omega) - f(U) + f(U) - \ell_{m-1} A^{m-1} - \ell_m A^m. \tag{3.9}$$

Finally, adding and subtracting ω_t and U_t gives the *error equation*

$$\rho_t - a\Delta\rho = f(\rho + \omega) - f(\omega) + f(\omega) - f(U) + R_T - \epsilon_t. \tag{3.10}$$

where R_T is the *temporal residual* given by $R_T := f(U) - \ell_{m-1} A^{m-1} - \ell_m A^m - U_t$ in I_m. It can be seen that R_T is expected to be of optimal order in time by substituting A^{m-1} and A^m. Moreover, we note that R_T is a computable quantity and its accuracy can always be verified numerically, cf., e.g., Example 3 in Section 6. Using the temporal residual, we then define the *time estimator* η_T^m on each time interval I_m by

$$\eta_T^m := \int_{I_m} ||R_T(s)|| \, \mathrm{d}s.$$

3.1. **Fixed Point Argument.** We now seek to show that (3.10) has a unique solution $\rho \in \mathcal{B}_m$ where $\mathcal{B}_m$ is the closed ball of radius $\delta_m \psi_m$ centered on zero in the $||\cdot||_m$ norm and where $\delta_m \in [1, \infty)$ is a parameter to be determined with ψ_m chosen such that

$$||\rho(t_{m-1})|| + \int_{I_m} ||\epsilon(s)|| \mathcal{L}(s, ||U(s)||, ||U(s)|| + ||\epsilon(s)||) \, \mathrm{d}s + \eta_T^m + \int_{I_m} ||\epsilon_t|| \, \mathrm{d}s \leq \psi_m, \tag{3.11}$$

where $\mathcal{L}$ is the local Lipschitz function from (1.2). The key idea here is that if we can show ρ exists in this ball then $||\rho||_m \leq \delta_m \psi_m$ were $\delta_m \psi_m$ is our computable *a posteriori* error estimator. Here, the term ψ_m contains local-in-time residuals which are of optimal order in space and time as well as the error estimator from the previous time step while δ_m, the solution of a nonlinear auxiliary equation, is a scaling parameter related to the nonlinearity which enforces the validity of the Banach Fixed Point Theorem (cf. (3.15) and (3.16) below). To prove the existence of $\rho \in \mathcal{B}_m$, we will use the Banach Fixed Point Theorem to show that Φ_m given by

$$\begin{aligned}\Phi_m(v)(t) := \mathrm{e}^{(t-t_{m-1})\Delta} \rho(t_{m-1}) + \int_{t_{m-1}}^t \mathrm{e}^{(t-s)\Delta} [f(v + \omega) - f(\omega) + f(\omega) - f(U)] \, \mathrm{d}s \\ + \int_{t_{m-1}}^t \mathrm{e}^{(t-s)\Delta} [R_T - \epsilon_t] \, \mathrm{d}s,\end{aligned}$$

$t \in \bar{I}_m$, has a unique fixed point $\rho \in \mathcal{B}_m$ which by Duhamel's Principle must also solve (3.10). To satisfy the criterea of the Banach Fixed Point Theorem, we must show two things:

(I) That Φ_m maps $\mathcal{B}_m$ onto itself.

(II) That Φ_m is a contraction mapping.

We begin the verification of these criteria by applying Theorem 3.1 to Φ_m. Thus for any $t \in \bar{I}_m$ and $v \in \mathcal{B}_m$ we have

$$||\Phi_m(v)(t)|| \leq ||\rho(t_{m-1})|| + \int_{t_{m-1}}^{t} ||f(v+\omega) - f(\omega)|| \, \mathrm{d}s + \int_{I_m} ||f(\omega) - f(U)|| \, \mathrm{d}s + \int_{I_m} ||R_T(s)|| \, \mathrm{d}s + \int_{I_m} ||\epsilon_t|| \, \mathrm{d}s.$$

Using (1.2) with the monotonicity of $\mathcal{L}$ and recalling (3.11) we obtain

$$||\Phi_m(v)(t)|| \leq \psi_m + \int_{t_{m-1}}^{t} ||v(s)|| \mathcal{L}(s, ||v(s)|| + ||U(s)|| + ||\epsilon(s)||, ||U(s)|| + ||\epsilon(s)||) \, \mathrm{d}s. \tag{3.12}$$

In order to bound this further, we require another lemma.

Lemma 3.13. *For any $t \in I_m$, the estimate*

$$||\epsilon(t)|| \leq \xi_m,$$

holds where $\xi_m := \max\{\mathcal{E}_{m-1}, \mathcal{E}_m\}$ with $\mathcal{E}_0 := ||u_0 - \mathcal{P}^1 u_0||$.

Proof. Since ϵ is linear in time, its maximal value occurs at either the left or right end point – the result then follows directly from Lemma 3.6 and upon recalling that $\epsilon(0) = e(0)$. □

Applying Lemma 3.13 to (3.12), using the monotonicity of $\mathcal{L}$ and noting that $v \in \mathcal{B}_m$ yields

$$||\Phi_m(v)||_m \leq \psi_m \left[1 + \delta_m \int_{I_m} L(s, \delta_m) \, \mathrm{d}s \right].$$

where

$$L(s, \delta) := \mathcal{L}(s, \delta\psi_m + ||U(s)|| + \xi_m, \delta\psi_m + ||U(s)|| + \xi_m), \qquad s \in I_m, \ \delta \in [1, \infty). \tag{3.14}$$

Thus we obtain that property (I) is satisfied if

$$1 + \delta_m \int_{I_m} L(s, \delta_m) \, \mathrm{d}s \leq \delta_m. \tag{3.15}$$

To show that property (II) holds, let $v_1, v_2 \in \mathcal{B}_m$ then the definition of Φ_m implies that

$$(\Phi_m(v_1) - \Phi_m(v_2))(t) = \int_{t_{m-1}}^{t} \mathrm{e}^{(t-s)\Delta} [f(v_1 + \omega) - f(v_2 + \omega)] \, \mathrm{d}s, \qquad t \in \bar{I}_m.$$

Applying Theorem 3.1 and Lemma 3.13 together with the monotonicity property of $\mathcal{L}$ and noting that $v_1, v_2 \in \mathcal{B}_m$ we obtain

$$\begin{aligned} ||(\Phi_m(v_1) - \Phi_m(v_2))(t)|| &\leq \int_{I_m} ||f(v_1 + \omega) - f(v_2 + \omega)|| \, \mathrm{d}s \\ &\leq \int_{I_m} ||(v_1 - v_2)(s)|| \mathcal{L}(s, ||v_1(s)|| + ||U(s)|| + ||\epsilon(s)||, ||v_2(s)|| + ||U(s)|| + ||\epsilon(s)||) \, \mathrm{d}s \\ &\leq \int_{I_m} L(s, \delta_m) ||(v_1 - v_2)(s)|| \, \mathrm{d}s. \end{aligned}$$

Therefore,

$$||\Phi_m(v_1) - \Phi_m(v_2)||_m \leq ||v_1 - v_2||_m \int_{I_m} L(s, \delta_m) \, \mathrm{d}s,$$

which is a contraction if

$$\int_{I_m} L(s, \delta_m) \, \mathrm{d}s < 1. \tag{3.16}$$

Note that (3.15) implies (3.16) since coupled with the fact that $\delta_m \in [1, \infty)$, (3.15) gives that

$$\int_{I_m} L(s, \delta_m) \, \mathrm{d}s \leq 1 - \delta_m^{-1} < 1.$$

Thus if (3.15) is satisfied then by the Banach Fixed Point Theorem, (3.10) has a unique solution $\rho \in \mathcal{B}_m$. As we have *choice* over the value δ_m can take in (3.15) then for practical reasons we choose $\delta_m \in [1, \infty)$ to be, if it exists, the *smallest* root of the function $\varphi_m : [1, \infty) \to \mathbb{R}$ defined by

$$\varphi_m(\delta) := 1 + \delta \left[\int_{I_m} L(s, \delta) \, \mathrm{d}s - 1 \right]. \tag{3.17}$$

Furthermore, we can in fact obtain a tighter bound on ρ under no additional assumptions. Indeed, we now know that if δ_m exists that $\Phi_m(\rho) = \rho \in \mathcal{B}_m$ satisfies (3.12); therefore, upon applying Gronwall's inequality and Lemma 3.13 to (3.12) we immediately deduce the bound

$$||\rho||_m \leq r_m \psi_m, \tag{3.18}$$

where $r_m \geq 1$ is given by

$$r_m = \exp\left(\int_{I_m} \mathcal{L}(s, \delta_m \psi_m + ||U(s)|| + \xi_m, ||U(s)|| + \xi_m) \, \mathrm{d}s \right). \tag{3.19}$$

Note that the upper bound in (3.18) is not yet computable as ψ_m is not yet an a posteriori quantity. We shall discuss this next.

Remark 3.20. With regards to blow-up problems, a natural question is how do we expect the multiplicative factor r_m to scale. Firstly, we observe numerically that $r_m \approx \delta_m$ for most time steps – this is not entirely unexpected since for $\int_{I_m} L(s, \delta_m) \, \mathrm{d}s$ small, (3.17) implies that

$$\delta_m = \frac{1}{1 - \int_{I_m} L(s, \delta_m) \, \mathrm{d}s} \approx 1 + \int_{I_m} L(s, \delta_m) \, \mathrm{d}s,$$

and so

$$r_m \approx 1 + \int_{I_m} \mathcal{L}(s, \delta_m \psi_m + ||U(s)|| + \xi_m, ||U(s)|| + \xi_m) \, \mathrm{d}s \approx 1 + \int_{I_m} L(s, \delta_m) \, \mathrm{d}s \approx \delta_m.$$

Then from numerical experiments for similar conditional ODE *a posteriori* error bounds [26] we would expect to observe that

$$\prod_{i=1}^{m} r_i \approx \prod_{i=1}^{m} \delta_i \propto \mathcal{F}(|T_\infty - t_m|^{-1}),$$

for some function $\mathcal{F} : \mathbb{R}_0^+ \to [1, \infty)$, $\lim_{x \to \infty} \mathcal{F}(x) = \infty$ dependent upon the nonlinearity f. We will further investigate this numerically for quadratic nonlinearities in the Numerical Experiments section (cf., e.g., Figure 1 below).

3.2. **Computable Error Bound.** Now that δ_m has been defined, we must characterize ψ_m from (3.11) in an *a posteriori* fashion in order to obtain a fully computable error bound. To do this, we must first estimate the term $||\rho(t_{m-1})||$ along with the remaining terms containing ϵ in (3.11).

In the previous subsection, we deduced that $\rho \in \mathcal{B}_m$ if δ_m exists; however, we assumed *a priori* knowledge of the existence of $\rho(t_{m-1})$ in (3.11). To rectify this, we note that for $m > 1$ we have

$$||\rho(t_{m-1})|| \leq ||\rho||_{m-1} \leq r_{m-1} \psi_{m-1}, \tag{3.21}$$

if $\rho \in \mathcal{B}_{m-1}$. Similarly, $\rho \in \mathcal{B}_{m-1}$ if δ_{m-1} exists and if we can verify the existence of $\rho(t_{m-2})$. Continuing this argument inductively, we see that $\rho \in \mathcal{B}_m$ provided that $\delta_1, \ldots, \delta_m$ exist.

With regards to the remaining terms in (3.11), the first term containing ϵ can be estimated directly by using the monotonicity of $\mathcal{L}$ combined with the bound of Lemma 3.13, viz.,

$$\int_{I_m} ||\epsilon(s)|| \mathcal{L}(s, ||U(s)||, ||U(s)|| + ||\epsilon(s)||) \, \mathrm{d}s \leq \xi_m \int_{I_m} \mathcal{L}(s, ||U(s)||, ||U(s)|| + \xi_m) \, \mathrm{d}s. \tag{3.22}$$

To bound ϵ_t term in (3.11), we require a lemma.

Lemma 3.23. *The following bound holds*

$$\int_{I_m} ||\epsilon_t|| \, ds \leq \xi'_m,$$

with

$$\xi'_m := \begin{cases} ||u_0 - \mathcal{P}^1 u_0|| + C_\infty \log(1/\underline{h}_m) \max\limits_{K\in\mathcal{T}_m} \eta_S^m\big|_K & \text{if } m = 1 \\ C_\infty \log(1/\widehat{\underline{h}}_m)\, k_m \max\limits_{\widehat{K}\in\mathcal{T}_{m-1}\wedge\mathcal{T}_m} \max\limits_{\check{K}\subseteq\widehat{K}} \dot{\eta}_S^m\big|_{\check{K}} & \text{if } m \geq 2 \end{cases},$$

where $\widehat{\underline{h}}_m := \min\{\underline{h}_{m-1}, \underline{h}_m\}$ *and where* $\dot{\eta}_S^m$ *is the space derivative estimator given by*

$$\dot{\eta}_S^m\big|_{\check{K}} := h_{\widehat{K}}^2 k_m^{-1} a^{-1} ||A^m - A^{m-1} + a\Delta(U^m - U^{m-1})||_{L^\infty(\check{K})} + h_{\widehat{K}} k_m^{-1} ||[\![\nabla(U^m - U^{m-1})]\!]||_{L^\infty(\partial\check{K}\setminus\partial\Omega)},$$

for $\mathcal{T}_{m-1} \vee \mathcal{T}_m \ni \check{K} \subseteq \widehat{K} \in \mathcal{T}_{m-1} \wedge \mathcal{T}_m$*. As before,* C_∞ *is a constant that is independent of the maximum mesh-size,* a*,* u *and* U *but may be dependent upon the size of the domain* Ω *as well as the number of refinement levels between* $\mathcal{T}_{m-1}$ *and* $\mathcal{T}_m$ *for* $m \geq 2$*.*

Proof. For $m = 1$, we have $\epsilon_t = (\epsilon(t_1) - e(0))/k_1$; the stated result then follows from the triangle inequality and Lemma 3.6. For $m \geq 2$, we note the observation made in Corollary 2.9 of [14] that ϵ_t is Galerkin orthogonal to the space $\mathcal{V}_h^{m-1} \cap \mathcal{V}_h^m$; the stated bound then follows by conducting the error analysis as in [13] but with a quasi-interpolant based on the mesh $\mathcal{T}_{m-1} \wedge \mathcal{T}_m$. □

Finally, applying the bounds of (3.21), (3.22) and Lemma 3.23 to the left-hand side of (3.11), we see that we can define ψ_m to be the computable *a posteriori* quantity given by

$$\psi_m := r_{m-1}\psi_{m-1} + \xi_m \int_{I_m} \mathcal{L}(s, ||U(s)||, ||U(s)|| + \xi_m)\, \mathrm{d}s + \eta_T^m + \xi'_m, \tag{3.24}$$

with the initial values $\psi_0 := 0$ and $r_0 := 1$. With ψ_m defined, all components of the error bound are now in place as well as fully computable and we are ready to state the main result.

Theorem 3.25. *Suppose that* $\delta_1, \ldots, \delta_M$ *the smallest roots of* (3.17) *in* $[1, \infty)$*, exist then the* $L^\infty L^\infty$ *error of the IMEX method* (2.2) *satisfies the a posteriori error bound*

$$\max_{1\leq m\leq M} ||e||_m \leq r_M \psi_M + \max_{1\leq m\leq M} \xi_m,$$

where r_M *and* ψ_M *are defined (for* $m = M$*) in* (3.19) *and* (3.24)*, respectively, and* ξ_m *is given in Lemma 3.13.*

Proof. Since $\delta_1, \ldots, \delta_M$ exist then by the exposition of the previous subsection we have

$$||\rho||_m \leq r_m \psi_m,$$

for any $1 \leq m \leq M$. Noting the decomposition $e = \rho + \epsilon$, we obtain that

$$\max_{1\leq m\leq M} ||e||_m \leq \max_{1\leq m\leq M} ||\rho||_m + \max_{1\leq m\leq M} ||\epsilon||_m \leq r_M \psi_M + \max_{1\leq m\leq M} ||\epsilon||_m.$$

The stated result then follows from Lemma 3.13. □

Given these results, a natural question to ask is whether $\delta_m \in [1, \infty)$, the smallest root of φ_m, can actually exist at all. This is the focus of our next lemma.

Lemma 3.26. *If* $\delta_0, \ldots, \delta_{m-1}$ *exist and the time step length* k_m *is chosen small enough then* φ_m *of* (3.17) *has a root in* $[1, \infty)$ *and thus the a posteriori error bound of Theorem 3.25 holds on* I_m*.*

Proof. We proceed along the same lines as Lemma 3.1 in [26]. Since $\delta_0, \ldots \delta_{m-1}$ exist, Theorem 3.25 implies that ψ_m exists and thus φ_m is well-defined. For fixed $\delta^\star > 1$ and upon setting $\epsilon = (\delta^\star - 1)/2 > 0$ we can choose $k_m > 0$ small enough so that

$$\delta^\star \int_{I_m} L(s, \delta^\star)\, \mathrm{d}s < 1 + \epsilon.$$

A quick calculation reveals that $\varphi_m(\delta^\star) < 1 + \epsilon - \delta^\star = (1 - \delta^\star)/2 = -\epsilon < 0$. Since φ_m is continuous and $\varphi_m(1) > 0$, it follows that for k_m sufficiently small φ_m has a root in $[1, \infty)$. □

We conclude this section by showing that the *a posteriori* error bound of Theorem 3.25 can be vastly simplified when f is independent of u.

Corollary 3.27. *Suppose that f is independent of u then the error of the IMEX method* (2.2) *unconditionally satisfies the a posteriori bound*

$$\max_{1\leq m\leq M}||e||_m \leq \sum_{m=1}^{M}\eta_T^m + \sum_{m=1}^{M}\xi_m' + \max_{1\leq m\leq M}\xi_m.$$

Proof. Since f is independent of u, it follows from (1.2) that $\mathcal{L}=0$. We recall that δ_m is the smallest root of the function $\varphi_m:[1,\infty)\to\mathbb{R}$ given by

$$\varphi_m(\delta) = 1+\delta\left[\int_{I_m} L(s,\delta)\,\mathrm{d}s - 1\right] = 1-\delta.$$

Therefore, $\delta_m = 1$ regardless of the size of the time step length k_m and so the *a posteriori* error bound of Theorem 3.25 holds unconditionally. The stated result then follows from Theorem 3.25 by applying ψ_m recursively and upon noting that $r_m = 1$. □

4. Adaptive Algorithms

In this section, we propose an adaptive algorithm that is based on the idea of minimization of the *a posteriori* error bound of Theorem 3.25. Ultimately, our goal is an adaptive algorithm that is applicable to both blow-up and fixed-time problems. Here, we consider an adaptive strategy that is based on using the residuals to control the time step lengths and mesh sizes but we emphasize that other adaptive strategies are possible for blow-up problems. For example, in [18], an existence analysis is carried out for implicit approximations to (1.1) via fixed point arguments and the results are used to select the length of the time steps in the scheme. A similar adaptive strategy could be used here in the sense that we could continue to reduce the size of the time step on I_m until δ_m exists and then fix this time step length before moving on to the next interval. Indeed, it was shown in [18] that choosing the size of the time steps in a way analagous to this can lead to superconvergence to the blow-up time; however, such a strategy does also come with certain disadvantages. Firstly, it is unclear how to generalize this approach to the case where f is independent of u since then δ_m *always* exists. Moreover, it is unclear what a 'natural' stop critereon for such an adaptive strategy should be whereas choosing the time step lengths according to the size of the residuals allows the non-existence of δ_m to be the stop critereon.

We contend that a general adaptive algorithm based on the *a posteriori* error bound of Theorem 3.25 should revert to a reasonable, well-known adaptive strategy when applied to a simple case such as that of Corollary 3.27. For this reason, we first outline an adaptive algorithm based on Corollary 3.27 and then extend this algorithm in a logical fashion to incorporate the full bound of Theorem 3.25. In what follows, we give a general outline of the idea behind the adaptive algorithms but for brevity we also include the pseudocode of the full algorithm in Algorithm 1.

4.1. Adaptive Algorithm for Corollary 3.27.

The nature of the data in Corollary 3.27 means that the algorithm in this subsection will be for a *fixed-time problem*. As such, the inputs to the algorithm include the data, the domain Ω, the final time T, a coarse initial mesh $\mathcal{T}_1$ of Ω and an unrefined initial time step length $k_1 \leq T$.

Suppose that we are on the generic time step $m>1$ then the backward solution $U^{m-1}\in\mathcal{V}_h^{m-1}$ and the mesh $\mathcal{T}_{m-1}$ are already fixed. To proceed on the current interval, we first set the mesh $\mathcal{T}_m = \mathcal{T}_{m-1}$ and then calculate the forward solution $U^m\in\mathcal{V}_h^m$ given by (2.2). The simple structure of the error bound immediately suggests defining the refinement indicators

$$\texttt{ref}_T^m := \eta_T^m, \qquad\qquad \texttt{ref}_S^m\big|_K := \max\Big\{\eta_S^m\big|_K, \dot{\eta}_S^m\big|_K\Big\},\ K\in\mathcal{T}_m.$$

Note that $\texttt{ref}_T^m$ is local to each time step while $\texttt{ref}_S^m$ is local to each mesh element. As is standard for spatial adaptivity done via L^∞ norm error estimates, we ignore the global logarithmic terms [36]. To control the size of the time steps and the mesh elements, we introduce four tolerances: a *spatial refinement tolerance* $\texttt{stol}^+$, a *spatial coarsening tolerance* $\texttt{stol}^-$, a *temporal refinement tolerance* $\texttt{ttol}^+$ and a *temporal coarsening tolerance* $\texttt{ttol}^-$. If necessary, we begin

by either refining or coarsening the time step length k_m and recalculating the forward solution $U^m \in \mathcal{V}_h^m$ until

$$\texttt{ttol}^- \leq \texttt{ref}_T^m \leq \texttt{ttol}^+,$$

is satisfied. We then fix this time step length. Next, we proceed spatially by, if permitted (see Remark 4.2 below), refining all elements $K \in \mathcal{T}_m$ such that $\texttt{ref}_S^m\big|_K > \texttt{stol}^+$ and coarsening all elements such that $\texttt{ref}_S^m\big|_K < \texttt{stol}^-$. We then recalculate (if necessary) and fix the forward solution $U^m \in \mathcal{V}_h^m$. After this is done, we set $k_{m+1} = k_m$ and proceed to the next interval unless the total time $t_{m+1} = t_m + k_{m+1}$ would surpass the final time T in which case we set $k_{m+1} = T - t_m$. When the final time is reached, we halt our computations.

All that remains is to deal with the coarse grid and time step length on the first interval. To do this, we must first modify the space refinement indicator in order to account for the unique form of ξ_m and ξ_m' on the first interval, viz.,

$$\texttt{ref}_S^1\big|_K := \max\left\{||u_0 - \mathcal{P}^1 u_0||_{L^\infty(K)},\, \eta_S^1\big|_K\right\},\ K \in \mathcal{T}_1.$$

Unfortunately, $\texttt{ref}_S^1$ is of a different form to $\texttt{ref}_S^m$ for $m > 1$ which can cause problems with spatial adaptivity; specifically, the mismatch between the spatial indicators can lead to excessive over-refinement between the first and second time steps. Our proposed solution to this issue is to introduce a constant $c_\star \leq 1$ such that

$$c_\star \approx \max_{K \in \mathcal{T}_1 (\equiv \mathcal{T}_2)} \frac{\texttt{ref}_S^1\big|_K}{\texttt{ref}_S^2\big|_K}.$$

This constant is used to weight the spatial tolerances on the first interval only, i.e., we refine elements $K \in \mathcal{T}_1$ such that $\texttt{ref}_S^1\big|_K > c_\star \texttt{stol}^+$ and coarsen elements such that $\texttt{ref}_S^1\big|_K < c_\star \texttt{stol}^-$. This ensures roughly equal parity between the spatial refinement indicators on all time steps.

To begin refinement of the course initial mesh/time step length, we first calculate the numerical solution $U^1 \in \mathcal{V}_h^1$ given by (2.2); we then proceed, via the tolerance strategy outlined above, by refining (or coarsening) the time step length k_1 and the mesh $\mathcal{T}_1$ concurrently then recalculating the numerical solution $U^1 \in \mathcal{V}_h^1$ until both $\texttt{ref}_T^1 \leq \texttt{ttol}^+$ and $\max_{K \in \mathcal{T}_1} \texttt{ref}_S^1\big|_K \leq c_\star \texttt{stol}^+$ are satisfied. After this is done, we set $k_2 = k_1$ and proceed to the next interval.

Remark 4.1. The refinement and coarsening tolerances need to be chosen sufficiently far apart so that the finite element solution does not get caught in an infinite refine and coarsen loop.

Remark 4.2. Numerical experiments show that the space derivative estimator $\dot{\eta}_S^m$ becomes temporarily unstable after mesh change has occured rendering its use in the spatial refinement indicator $\texttt{ref}_S^m$ problematic. There are two practical ways to address this issue and prevent runaway degradation of the FEM solution: we can remove $\dot{\eta}_S^m$ from the spatial refinement indicator altogether or we can restrict mesh change to every few time steps in order to allow $\dot{\eta}_S^m$ time to normalize. We opt for the second approach and only allow mesh change every n time steps as we consider this more desirable than the alternative which would involve excluding potential solution information from the spatial refinement indicator.

4.2. **Adaptive Algorithm for Theorem 3.25.** In this subsection, we modify the adaptive algorithm of the previous subsection for adaptivity under the full estimator of Theorem 3.25; we do this in such a way that the algorithm of the previous subsection is recovered when f is independent of u. In fact, the only changes that need to be made to the algorithm of the previous subsection are:

(1) The stop critereon must be altered to account for the fact that the error bound may now not necessarily hold.

(2) The refinement indicators must be modified for adaptivity under the full error estimator.

To address point (1), we recall from Theorem 3.25 that the error bound holds on I_m provided that $\delta_1, \ldots, \delta_m$ exist; therefore, after all the adaptive procedures on the current interval are complete, we attempt to calculate δ_m via a root-finding algorithm. If we find a root then we continue to the next interval (unless the final time is reached); if not, we halt our computations.

A naïve approach towards addressing point (2) would be to simply use the refinement indicators of the previous subsection for adaptivity, however, doing so not only completely ignores the structure of the error estimator but also the length scales inherent to a blow-up problem. Consequently, such a refinement indicator causes excessive over-refinement close to the blow-up time which, in turn, results in suboptimal convergence [9, 26, 31]. In order to characterize the new refinement indicators, we define

$$\widetilde{r}_m := \prod_{i=0}^{m} r_i,$$

to be the accumulation of the values r_i, $0 \leq i \leq m$. We remark that $\widetilde{r}_m$ is a value intimately connected with the rate of blow-up of the exact solution on the interval $(0, t_m)$ as shown in the numerical experiments of [26] and as we shall show here in the sequel; therefore, it is natural that this quantity should appear in our refinement indicators.

With this notation at hand, the temporal refinement indicator is given by

$$\texttt{ref}_T^m := \widetilde{r}_{m-1}^{-1} \eta_T^m.$$

For a rigorous justification of this choice, we refer the reader to [26]. Defining the space refinement indicator is more involved as reviewing the error bound of Theorem 3.25, it is clear that some terms are affected by r_m while others are not. The lone spatial term outside the recursive portion of the error bound is independent of r_m which suggests that we demand that

$$\eta_S^m\big|_K \leq \texttt{stol}^+, \ K \in \mathcal{T}_m, \tag{4.3}$$

is satisfied. On the other hand, the space derivative estimator $\dot{\eta}_S^m$ is part of the term ψ_m which is affected by r_m and so we ask that

$$\widetilde{r}_{m-1}^{-1} \dot{\eta}_S^m\big|_K \leq \texttt{stol}^+, \ K \in \mathcal{T}_m, \tag{4.4}$$

is satisfied. The remaining spatial term in ψ_m is affected by r_m as well but we must also divide it by the time step length k_m in order to incorporate it into the space refinement indicator as the space refinement indicator shouldn't be (strongly) dependent upon the time step length. Therefore, we require that

$$\left[\widetilde{r}_{m-1}^{-1} k_m^{-1} \int_{I_m} \mathcal{L}(s, ||U(s)||, ||U(s)|| + \xi_m) \, \mathrm{d}s\right] \eta_S^m\big|_K \leq \texttt{stol}^+, \ K \in \mathcal{T}_m, \tag{4.5}$$

is satisfied. So upon defining

$$\alpha_m := \max\left\{1, \widetilde{r}_{m-1}^{-1} k_m^{-1} \int_{I_m} \mathcal{L}(s, ||U(s)||, ||U(s)|| + \xi_m) \, \mathrm{d}s\right\},$$

we combine (4.3), (4.4) and (4.5) to define the space refinement indicator (for $m > 1$), viz.,

$$\texttt{ref}_S^m\big|_K := \max\left\{\alpha_m \eta_S^m\big|_K, \widetilde{r}_{m-1}^{-1} \dot{\eta}_S^m\big|_K\right\}, \ K \in \mathcal{T}_m.$$

As in the previous subsection, we must again modify the space refinement indicator on the first interval in order to account for the unique form of ξ_m and ξ_m' on that interval, viz.,

$$\texttt{ref}_S^1\big|_K := \max\left\{\alpha_1 ||u_0 - \mathcal{P}_1 u_0||_{L^\infty(K)}, \alpha_1 \eta_S^1\big|_K\right\}, \ K \in \mathcal{T}_1.$$

Finally, we recall from Corollary 3.27 that for f independent of u we have $\mathcal{L} = 0$ and $\delta_m = 1$. As δ_m always exists for this type of data, the additional stop critereon introduced in this subsection never comes into play. Moreover, $\mathcal{L} = 0$ implies $\widetilde{r}_m = 1$ and so the reference indicators introduced here for the general case devolve into those of the previous subsection for f independent of u. Therefore, we conclude that the two adaptive algorithms are the same for this type of data.

Algorithm 1 Space-time adaptivity for the semilinear heat equation

Input: a, f, u_0, Ω, T, $\mathcal{T}_1$, k_1, $c_\star$, n, $\texttt{stol}^+$, $\texttt{stol}^-$, $\texttt{ttol}^+$, $\texttt{ttol}^-$.
Compute U^1.
while $\texttt{ref}_T^1 > \texttt{ttol}^+$ **or** $\max_{K\in\mathcal{T}_1} \texttt{ref}_S^1\big|_K > c_\star\texttt{stol}^+$ **do**
    Modify $\mathcal{T}_1$ by refining all elements such that $\texttt{ref}_S^1\big|_K > c_\star\texttt{stol}^+$ and coarsening all elements such that $\texttt{ref}_S^1\big|_K < c_\star\texttt{stol}^-$.
    if $\texttt{ref}_T^1 > \texttt{ttol}^+$ **then**
        $k_1 \leftarrow k_1/2$.
    end if
    Compute U^1.
end while
Attempt to compute δ_1.
Set $m = 0$.
while δ_{m+1} exists **and** $t_{m+1} < T$ **do**
    $m \leftarrow m + 1$.
    Set $\mathcal{T}_{m+1} = \mathcal{T}_m$ and $k_{m+1} = \min\{k_m, T - t_m\}$.
    Compute U^{m+1} from U^m.
    if $\texttt{ref}_T^{m+1} > \texttt{ttol}^+$ **then**
        $k_{m+1} \leftarrow k_{m+1}/2$.
        Compute U^{m+1} from U^m.
    end if
    if $\texttt{ref}_T^{m+1} < \texttt{ttol}^-$ **then**
        $k_{m+1} \leftarrow \min\{2k_{m+1}, T - t_m\}$.
        Compute U^{m+1} from U^m.
    end if
    if $m \bmod n = 0$ **then**
        Modify $\mathcal{T}_{m+1}$ by refining all elements such that $\texttt{ref}_S^{m+1}\big|_K > \texttt{stol}^+$ and coarsening all elements such that $\texttt{ref}_S^{m+1}\big|_K < \texttt{stol}^-$.
        Compute U^{m+1} from U^m.
    end if
    Attempt to compute δ_{m+1}.
end while
if δ_{m+1} exists **and** $t_{m+1} = T$ **then**
    $m \leftarrow m + 1$.
end if
Output: m, t_m, U, $r_m\psi_m$.

5. Numerical Experiments

We consider an implementation of the adaptive algorithm of the previous section through an application of the `deal.II` finite element library [3, 4]. For all of the numerical experiments, we only allow the mesh to change every three time steps. In order to facilitate a comparison between the $L^\infty L^\infty$ estimator of Theorem 3.25 and the L^2H^1 estimator of [9], we consider Example 1 and Example 3 of [9] but under the adaptive algorithm of the previous section driven by the $L^\infty L^\infty$ *a posteriori* error bound derived in this paper. If the *a posteriori* error bound of Theorem 3.25 is robust with respect to the distance from the blow-up time then for sufficiently small $\texttt{stol}^+$ and $\texttt{stol}^-$, we would expect to observe that

$$|T_\infty - T(\texttt{ttol}^+, N)| \propto N^{-1},$$

where T_∞ is the blow-up time of (1.1) and T is the final time produced by the adaptive algorithm in N total time steps under a given temporal refinement tolerance $\texttt{ttol}^+$ as this is what was observed in the ODE experiments of [9, 26, 31]. Additionally, we also apply the adaptive algorithm

to a nonlinear fixed-time problem in order to demonstrate its generality and to show that the estimator of Theorem 3.25 is of optimal order in space and time.

5.1. **Example 1.** Let $\Omega = (-8,8)^2$, $a = 1$, $f(u) = u^2$ and choose the initial condition to be the Gaussian blob given by $u_0(x,y) = 10\exp(-2x^2 - 2y^2)$. The blow-up set for this example consists of only a single point (the origin) making it spatially uncomplicated which allows us to focus solely on the temporal asymptotics. Now, since $f(u) = u^2$ then for any $v_1, v_2 \in \mathbb{R}$ we have

$$|f(v_1) - f(v_2)| = |v_1^2 - v_2^2| \leq |v_1 - v_2|(|v_1| + |v_2|).$$

Therefore, we have $\mathcal{L}(|v_1|,|v_2|) = |v_1| + |v_2|$ in (1.2) and so δ_m (if it exists) is the smallest root of the function $\varphi_m : [1,\infty) \to \mathbb{R}$ given by

$$\varphi_m(\delta) = 1 + \delta\left[\int_{I_m} L(s,\delta)\,\mathrm{d}s - 1\right] = 1 + \delta\left[2k_m\xi_m + 2\int_{I_m} ||U(s)||\,\mathrm{d}s - 1\right] + 2k_m\psi_m\delta^2. \quad (5.1)$$

In this case, we can calculate δ_m explicitly via the quadratic formula and so there is no need to use a root finding algorithm here.

Given that we are primarily interested in observing temporal behaviour, we opt to use high degree polynomials (degree nine specifically) to minimize the spatial error. We begin by first setting a small spatial refinement tolerance $\texttt{stol}^+$ so that the spatial error is negligible; we then gradually reduce the temporal refinement tolerance $\texttt{ttol}^+$ in order to observe the rate of convergence to the blow-up time. We include the results in the left-hand side of Table 1 alongside the results that utilize the L^2H^1 estimator of [9] on the right-hand side.

TABLE 1. Example 1: $L^\infty L^\infty$ estimator of Theorem 3.25 (left) and L^2H^1 estimator of [9] (right).

$\texttt{ttol}^+$	Time Steps	Final Time	$\|\|U(T)\|\|$
0.25	2	0.05375	11.045
0.25^2	9	0.12094	14.611
0.25^3	23	0.15453	19.941
0.25^4	52	0.17469	27.729
0.25^5	114	0.19148	42.965
0.25^6	397	0.20366	77.976
0.25^7	816	0.20933	130.275
0.25^8	1655	0.21227	208.52
0.25^9	3339	0.21421	347.669
0.25^{10}	6711	0.21537	584.525
0.25^{11}	13460	0.21606	998.835

Time Steps	Final Time	$\|\|U(T)\|\|$
3	0.09375	12.244
8	0.12500	14.742
19	0.14844	18.556
42	0.16406	23.468
92	0.17969	32.108
195	0.19043	44.217
405	0.19775	60.493
832	0.20313	83.315
1698	0.20728	117.780
3443	0.21014	165.833
6956	0.21228	238.705
14008	0.21375	343.078
28151	0.21478	496.885
56489	0.21549	722.884

The results show that for this example the $L^\infty L^\infty$ estimator of Theorem 3.25 outperforms the L^2H^1 estimator of [9] in terms of rate of convergence to the blow-up time. We recall from [9] that given two consecutive data points we can approximate the exact blow-up time T_∞ as follows

$$T_\infty \approx \frac{t_m||U^m|| - t_{m-1}||U^{m-1}||}{||U^m|| - ||U^{m-1}||}. \quad (5.2)$$

Applying this here, we obtain the approximation $T_\infty \approx 0.217015$. Using this approximation to T_∞, we take the data from Table 1 and plot the distance from the blow-up time $|T - T_\infty|$ versus the total number of time steps N in Figure 1. The plot shows that for this example we have

$$|T_\infty - T(\texttt{ttol}^+, N)| \propto N^{-3/4}.$$

This is slightly slower than expected given the ODE results of [9, 26, 31]. Finally, for the final computational run we plot the magnitude of the numerical solution $||U(t)||$, the parabolic estimator

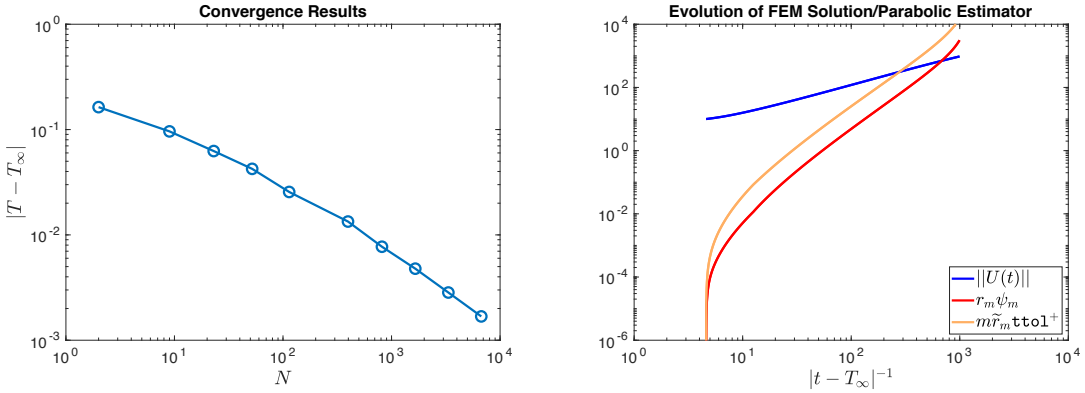

FIGURE 1. Example 1: convergence results (left) and evolution of the numerical solution (right).

$r_m\psi_m$ and the value $m\widetilde{r}_m\texttt{ttol}^+$ versus the inverse of the distance to the blow-up time. From the results, given in Figure 1, we deduce the asymptotic estimate

$$||U(t)|| \propto |t - T_\infty|^{-1},$$

which is consistent with the asymptotics of the exact solution [29,30] suggesting that our numerical solution is reasonable. Moreover, we expect (cf. Corollary 4.3 of [26]) that in the spatially asymptotic regime and under the adaptive strategy induced by the adaptive algorithm that the parabolic error ρ satisfies

$$\max_{1\leq k\leq m} ||\rho||_k \leq r_m\psi_m \leq m\widetilde{r}_m\texttt{ttol}^+,$$

which we confirm in Figure 1. Therefore, upon observing that the gradient of the estimator curves in Figure 1 is two, we deduce that there exists a constant $C > 0$ that is independent of the distance to the blow-up time such that

$$\max_{1\leq k\leq m} ||\rho||_k \leq C|t_m - T_\infty|^{-2}.$$

5.2. **Example 2.** Let $\Omega = (-8, 8)^2$, $a = 1$, $f(u) = u^2$ and the "volcano" type initial condition be given by $u_0(x, y) = 10(x^2 + y^2)\exp(-0.5x^2 - 0.5y^2)$. The blow-up set for this example is a circle centered on the origin making this example a good test of the spatial capabilities of the adaptive algorithm as many degrees of freedom are required in order to resolve the one-dimensional singularity close to the blow-up time. We remark that as the nonlinearity here is the same as in Example 1, δ_m is again the smallest root of (5.1).

For this example, we again opt to use polynomials of degree nine in order to observe the temporal asymptotics. We proceed as in the previous example by choosing a small spatial refinement tolerance $\texttt{stol}^+$ so that the spatial error is negligible; we then gradually reduce the temporal refinement tolerance $\texttt{ttol}^+$ in order to observe the rate of convergence to the blow-up time. The results, displayed on the left-hand side of Table 2 alongside the results that utilize the L^2H^1 estimator of [9] on the right-hand side, show that the $L^\infty L^\infty$ estimator of Theorem 3.25 again outperforms the L^2H^1 estimator of [9] by an order of magnitude.

As the nonlinearity is the same here as in Example 1, (5.2) is still valid and so we obtain the approximation $T_\infty \approx 0.166460$. Using this approximation to T_∞, we take the data from Table 2 and plot the distance from the blow-up time $|T - T_\infty|$ versus the total number of time steps N in Figure 2. The plot shows that for this example we have

$$|T_\infty - T(\texttt{ttol}^+, N)| \propto N^{-1},$$

which is what we expected to observe given the ODE results of [9, 26, 31]. Next, we investigate the spatial properties of the adaptive algorithm during the final computational run. We begin by plotting the number of degrees of freedom versus the inverse of the distance to the blow-up time in Figure 2. The plot shows a general (non-excessive) increase in the number of degrees of freedom

TABLE 2. Example 2: $L^\infty L^\infty$ estimator of Theorem 3.25 (left) and L^2H^1 estimator of [9] (right).

$\texttt{ttol}^+$	Time Steps	Final Time	$\|\|U(T)\|\|$
0.25	4	0.08280	12.005
0.25^2	11	0.11385	17.687
0.25^3	26	0.13455	27.548
0.25^4	71	0.15525	65.557
0.25^5	159	0.16043	119.261
0.25^6	333	0.16334	221.442
0.25^7	714	0.16512	476.916
0.25^8	1470	0.16572	881.210
0.25^9	2978	0.16607	1648.860
0.25^{10}	6120	0.16628	3508.360
0.25^{11}	12336	0.16637	6663.990
0.25^{12}	24938	0.16641	13241.900

Time Steps	Final Time	$\|\|U(T)\|\|$
3	0.06250	10.371
10	0.09375	14.194
36	0.11979	21.842
86	0.13412	31.446
190	0.14388	45.122
404	0.15072	64.907
880	0.15601	98.048
1853	0.15942	146.162
3831	0.16176	219.423
7851	0.16336	332.849
16137	0.16442	505.236
32846	0.16512	769.652
66442	0.16558	1175.210

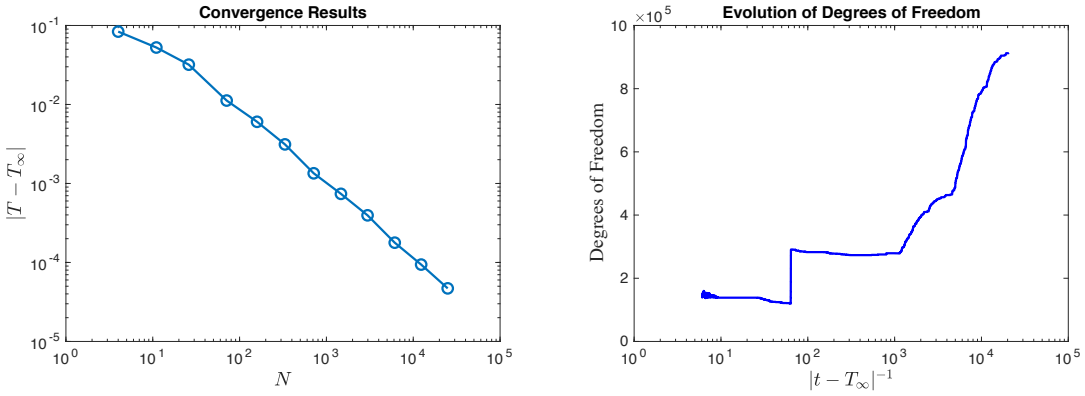

FIGURE 2. Example 2: convergence results (left) and evolution of degrees of freedom (right).

as we advance towards the blow-up time with some local decreases. To investigate this further, we display the meshes at times $t = 0$ and $t = T$ in Figure 3 which shows heavy refinement has occured around the blow-up set with some derefinement in areas from which the finite element solution has retreated. For visualization purposes, we also display profile views of the finite element solution at times $t = 0$ and $t = T$ in Figure 3.

5.3. **Example 3.** In this example, we consider a nonlinear parabolic problem from [2,38]. We set $\Omega = (0,1)^2$, $T = 0.5$, $a = 0.001$, $f(t,u) = \sin(t) - u^4$ and $u_0(x,y) = xy(x-1)(y-1)$. The solution is initially unremarkable but as time advances it begins to exhibit boundary layers through the influence of the diffusion and the forcing term. For this nonlinearity, given any $t \in [0,T]$ and $v_1, v_2 \in \mathbb{R}$ we have

$$|f(t,v_1) - f(t,v_2)| = |v_1^4 - v_2^4| \leq |v_1 - v_2|(|v_1|^3 + |v_1|^2|v_2| + |v_1||v_2|^2 + |v_2|^3).$$

Therefore, we have $\mathcal{L}(|v_1|,|v_2|) = |v_1|^3 + |v_1|^2|v_2| + |v_1||v_2|^2 + |v_2|^3$ in (1.2) and so δ_m (if it exists) is the smallest root of the function $\varphi_m : [1,\infty) \to \mathbb{R}$ given by

$$\varphi_m(\delta) = 1 + \delta\left[\int_{I_m} L(s,\delta)\,\mathrm{d}s - 1\right] = 1 - \delta + 4\delta\int_{I_m} (\delta\psi_m + ||U(s)|| + \xi_m)^3\,\mathrm{d}s,$$

which we approximate via a Newton method.

Our primary goal in this numerical example is to verify that the estimator of Theorem 3.25 is of optimal order in space and time when applied to a fixed-time problem. To that end, we begin by

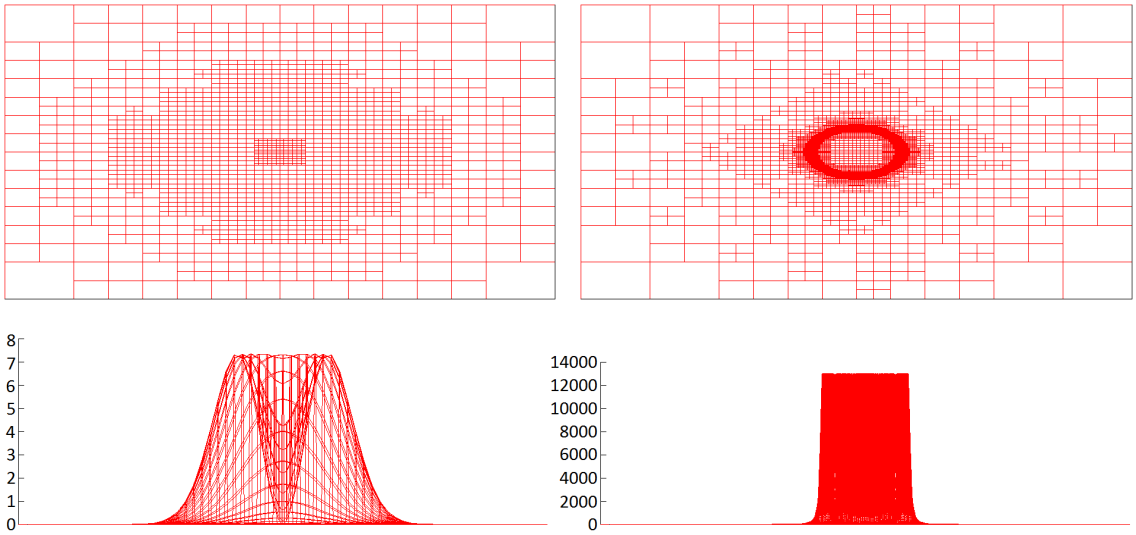

FIGURE 3. Example 2: initial mesh (top left), final mesh (top right), initial solution profile (bottom left) and final solution profile (bottom right).

first checking the rate of convergence of the estimator in time. To do this, we choose polynomials of degree nine and a small spatial refinement tolerance $\texttt{stol}^+$ so that the spatial contribution to the estimator is negligible; we then gradually reduce the temporal refinement tolerance $\texttt{ttol}^+$ in order to observe the rate of convergence of the estimator in time. For each computational run, we then plot the value of the estimator at final time versus the total number of time steps. The results, displayed in Figure 4, show that the estimator is order one in time and, hence, optimal.

To analyze the rate of convergence of the estimator in space, we need to introduce a concept from [10] which is that of the *weighted average degrees of freedom* given by

$$\text{weighted average dofs} := \frac{1}{T}\sum_{m=1}^{M} k_m \times \#\,\text{dofs}\,(\mathcal{T}_m).$$

In order to observe the rate of convergence of the estimator in space, we first choose a small temporal refinement tolerance $\texttt{ttol}^+$ so that the size of the temporal contribution to the estimator is negligible; we then gradually reduce the spatial refinement tolerance $\texttt{stol}^+$ for polynomials of degree three and, for each computation, plot the value of the estimator at final time versus the weighted average degrees of freedom. The results, given in Figure 4, show that the spatial convergence is quite nonlinear but that we obtain the expected, optimal rate of convergence when the rate is calculated over all the computational runs. We also display the meshes from one of the computational runs at times $t = 0$ and $t = T$ in Figure 5. The initial mesh displays refinement around the boundary suggesting that the spatial estimator has correctly anticipated the formation of boundary layers. In the final mesh, we see that there is much heavier refinement around the boundary than in the initial mesh implying that the spatial estimator has accurately captured the evolution of the boundary layers as they formed.

6. Conclusions

We derived a conditional $L^\infty L^\infty$ *a posteriori* error bound (Theorem 3.25) for the IMEX discretization (2.2) of the semilinear heat equation (1.1) with the general local Lipschitz nonlinearity (1.2). Our numerical experiments indicate that the proposed estimator outperforms the L^2H^1 estimator of [9] with respect to estimation of the blow-up time. Moreover, we were able to ascertain that the rate of convergence to the blow-up time is order one in the best-case scenario (Example 2) but we also determined that it can be slower (albeit still faster than in [9]) in certain situations (Example 1). The slow convergence in Example 1 can be explained by the initial condition not

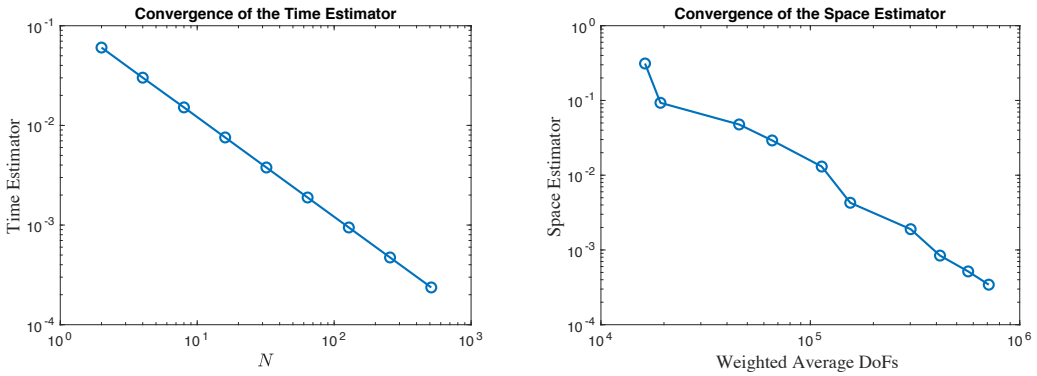

FIGURE 4. Example 3: temporal convergence (left) and spatial convergence for $p = 3$ (right).

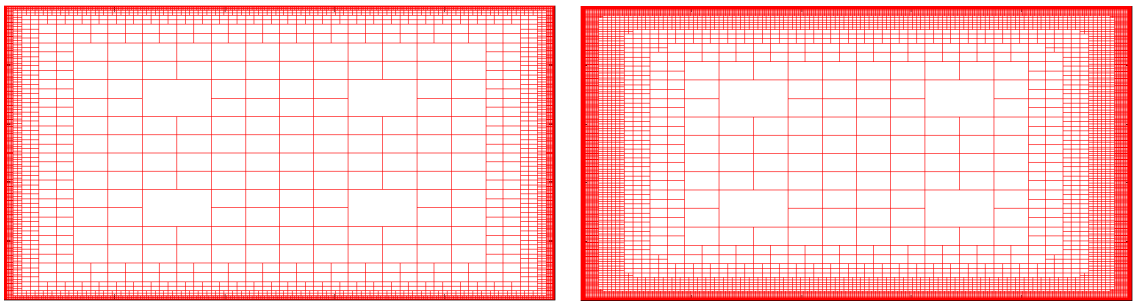

FIGURE 5. Example 3: initial mesh (left) and final mesh (right).

having a "compatible profile" with the blow-up, that is, this choice of initial condition causes the solution to be significantly influenced by the laplacian early on (this can be seen in Figure 1 by noting that the numerical solution only achieves the estimate $||U(t)|| \propto |t - T_\infty|^{-1}$ asymptotically and not at all stages of the computation) in a way that is not suitably accounted for by the proposed estimator. Attempts were made to modify the estimator of Theorem 3.25 to account for the influence of the laplacian in the spirit of Proposition 4.5 of [14] but this did not appear to have a significant impact on the performance of the estimator. We note, however, that a requirement on the initial condition to have a "compatible profile" with the nonlinearity in order to achieve optimal convergence is not unreasonable and has been a requirement in the *a posteriori* error analysis of other nonlinear problems, for example, in [21]. Additionally, we verified in Example 3 that the estimator is of optimal order in space and time when applied to a fixed-time problem. Finally, we remark that condition (1.2) is very general and that the estimator of Theorem 3.25 can, in principle, be applied to *any* nonlinear problem which satisfies it. In practise, however, the exponential term $\widetilde{r}_m$ restricts application of the estimator to nonlinear problems for which either

(1) the initial condition is small or,

(2) the nonlinearity is small or,

(3) the final time is small.

This also shows why the estimator works well for blow-up problems – because a large nonlinearity corresponds to a small blow-up time ensuring that $\widetilde{r}_m$ never grows out of control. In the future, we would like to robustly incorporate the influence of the laplacian into the estimator of Theorem 3.25, prove convergence to the blow-up time under the proposed adaptive algorithm and explore the possibility of exponential convergence to the blow-up time in the spirit of [26].

7. Acknowledgements

The research in this paper was conducted while the second author was affiliated with Universität Bern and he is thankful to them for supporting the research. The authors would also like to thank Prof. Thomas P. Wihler of Universität Bern for his comments and insights.

References

1. Gabriel Acosta, Ricardo G. Durán, and Julio D. Rossi, *An adaptive time step procedure for a parabolic problem with blow-up*, Computing **68** (2002), no. 4, 343–373.
2. Mario Amrein and Thomas P. Wihler, *An adaptive space-time Newton–Galerkin approach for semilinear singularly perturbed parabolic evolution equations*, IMA Journal of Numerical Analysis (2016), drw049.
3. Wolfgang Bangerth, Denis Davydov, Timo Heister, Luca Heltai, Guido Kanschat, Martin Kronbichler, Matthias Maier, Bruno Turcksin, and David Wells, *The `deal.II` library, version 8.4*, Journal of Numerical Mathematics **24** (2016).
4. Wolfgang Bangerth, Ralf Hartmann, and Guido Kanschat, *deal.ii – a general-purpose object-oriented finite element library*, ACM Transactions on Mathematical Software (TOMS) **33** (2007), no. 4, 24.
5. Eberhard Bänsch, Fotini Karakatsani, and Charalambos Makridakis, *The effect of mesh modification in time on the error control of fully discrete approximations for parabolic equations*, Applied Numerical Mathematics **67** (2013), 35–63.
6. Sören Bartels, *A posteriori error analysis for time-dependent Ginzburg-Landau type equations*, Numer. Math. **99** (2005), no. 4, 557–583.
7. Marsha Berger and Robert V. Kohn, *A rescaling algorithm for the numerical calculation of blowing-up solutions*, Comm. Pure Appl. Math. **41** (1988), no. 6, 841–863.
8. Chris J. Budd, Weizhang Huang, and Robert D. Russell, *Moving mesh methods for problems with blow-up*, SIAM J. Sci. Comput. **17** (1996), no. 2, 305–327.
9. Andrea Cangiani, Emmanuil H. Georgoulis, Irene Kyza, and Stephen Metcalfe, *Adaptivity and blow-up detection for nonlinear evolution problems*, SIAM Journal on Scientific Computing **38** (2016), no. 6, A3833–A3856.
10. Andrea Cangiani, Emmanuil H. Georgoulis, and Stephen Metcalfe, *Adaptive discontinuous Galerkin methods for nonstationary convection–diffusion problems*, IMA Journal of Numerical Analysis (2013), drt052.
11. Andrea Cangiani, Emmanuil H. Georgoulis, Andrew Y. Morozov, and Oliver J. Sutton, *Revealing new dynamical patterns in a reaction-diffusion model with cyclic competition via a novel computational framework*, Proceedings of the Royal Society A: Mathematical, Physical and Engineering Sciences **474** (2018), no. 2213, 20170608.
12. Eduardo Cuesta and Charalambos Makridakis, *A posteriori error estimates and maximal regularity for approximations of fully nonlinear parabolic problems in Banach spaces*, Numer. Math. **110** (2008), 257–275.
13. Alan Demlow and Natalia Kopteva, *Maximum-norm a posteriori error estimates for singularly perturbed elliptic reaction-diffusion problems*, Numerische Mathematik (2014), 1–36.
14. Alan Demlow, Omar Lakkis, and Charalambos Makridakis, *A posteriori error estimates in the maximum norm for parabolic problems*, SIAM Journal on Numerical Analysis **47** (2009), no. 3, 2157–2176.
15. Todd Dupont, *Mesh modification for evolution equations*, Math. Comp. **39** (1982), no. 159, 85–107. MR 658215 (84g:65131)
16. Emmanuil H. Georgoulis and Charalambos Makridakis, *On a posteriori error control for the Allen-Cahn problem*, Math. Method. Appl. Sci. **37** (2014), no. 2, 173–179.
17. Pablo Groisman, *Totally discrete explicit and semi-implicit euler methods for a blow-up problem in several space dimensions*, Computing **76** (2006), no. 3–4, 325–352.
18. Bärbel Holm and Thomas P. Wihler, *Continuous and discontinuous Galerkin time stepping methods for nonlinear initial value problems with application to finite time blow-up*, Numerische Mathematik (2017).
19. Bei Hu, *Blow-up theories for semilinear parabolic equations*, Lecture Notes in Mathematics, vol. 2018, Springer, Heidelberg, 2011.
20. Weizhang Huang, Jingtang Ma, and Robert D. Russell, *A study of moving mesh PDE methods for numerical simulation of blowup in reaction diffusion equations*, J. Comput. Phys. **227** (2008), no. 13, 6532–6552.
21. Daniel Kessler, Ricardo H. Nochetto, and Alfred Schmidt, *A posteriori error control for the Allen-Cahn problem: circumventing Gronwall's inequality*, ESAIM Math. Model. Numer. Anal. **38** (2004), no. 1, 129–142 (eng).
22. Natalia Kopteva and Torsten Linss, *Maximum norm a posteriori error estimation for parabolic problems using elliptic reconstructions*, SIAM Journal on Numerical Analysis **51** (2016), no. 3, 1494–1524.
23. ———, *Improved maximum-norm a posteriori error estimates for linear and semilinear parabolic equations*, Advances in Computational Mathematics (2017).
24. Irene Kyza, *A posteriori error estimates for approximations of semilinear parabolic and Schrödinger-type equations*, PhD Thesis, University of Crete (2009).
25. Irene Kyza and Charalambos Makridakis, *Analysis for time discrete approximations of blow-up solutions of semilinear parabolic equations*, SIAM J. Numer. Anal. **49** (2011), no. 1, 405–426.
26. Irene Kyza, Stephen Metcalfe, and Thomas P. Wihler, *hp-adaptive Galerkin time stepping methods for nonlinear initial value problems*, Journal of Scientific Computing **75** (2018), 111–127.

27. Omar Lakkis and Charalambos Makridakis, *Elliptic reconstruction and a posteriori error estimates for fully discrete linear parabolic problems*, Math. Comp. **75** (2006), no. 256, 1627–1658. MR 2240628 (2007e:65122)
28. Charalambos Makridakis and Ricardo H. Nochetto, *Elliptic reconstruction and a posteriori error estimates for parabolic problems*, SIAM J. Numer. Anal. **41** (2003), no. 4, 1585–1594. MR 2034895 (2004k:65157)
29. Frank Merle and Hatem Zaag, *Optimal estimates for blowup rate and behavior for nonlinear heat equations*, Comm. Pure Appl. Math. **51** (1998), no. 2, 139–196.
30. ———, *A Liouville theorem for vector-valued nonlinear heat equations and applications*, Math. Ann. **316** (2000), no. 1, 103–137.
31. Stephen Metcalfe, *Adaptive discontinuous Galerkin methods for nonlinear parabolic problems*, PhD Thesis, University of Leicester (2015).
32. Makoto Mizuguchi, Akitoshi Takayasu, Takayuki Kubo, and Shinichi Oishi, *Accurate method of verified computing for solutions of semilinear heat equations*, Reliable Computing **25** (2017), 74–99 (English).
33. ———, *A method of verified computations for solutions to semilinear parabolic equations using semigroup theory*, SIAM Journal on Numerical Analysis **55** (2017), no. 2, 980–1001.
34. ———, *Numerical verification for existence of a global-in-time solution to semilinear parabolic equations*, Journal of Computational and Applied Mathematics **315** (2017), 1–16.
35. Van Tien Nguyen and Hatem Zaag, *Blow-up results for a strongly perturbed semilinear heat equation: Theoretical analysis and numerical method*, Analysis & PDE **9** (2016), no. 1, 229–257.
36. Ricardo H. Nochetto, Alfred Schmidt, Kunibert G. Siebert, and Andreas Veeser, *Pointwise a posteriori error estimates for monotone semi-linear equations*, Numerische Mathematik **104** (2006), no. 4, 515–538.
37. Vidar Thomée, *Galerkin finite element methods for parabolic problems*, vol. 1054, Springer, 1984.
38. Ferdinand Verhulst, *Methods and applications of singular perturbations: boundary layers and multiple timescale dynamics*, vol. 50, Springer Science & Business Media, 2005.

Department of Mathematics, University of Dundee, Dundee, DD1 4HN, United Kingdom
Email address: ikyza@dundee.ac.uk

Department of Mechanical Engineering, McGill University, Montréal, H3A 0C3, Canada
Email address: smetcalfephd@gmail.com